RESEARCH ARTICLE

INTERNATIONAL RESEARCH JOURNAL OF MULTIDISCIPLINARY TECHNOVATION

Asian Research Association

DOI: 10.54392/irjmt24316

Early Diagnosis of Lung Infection via Deep Learning Approach

Marwa A. Shames [a], Mohammed Y. Kamil [a, *]

[a] Department of Physics, College of Science, Mustansiriyah University, Baghdad, Iraq

*Corresponding Author Email: m80y98@uomustansiriyah.edu.iq

DOI: https://doi.org/10.54392/irjmt24316

Received: 28-12-2023; Revised: 20-04-2024; Accepted: 03-05-2024; Published: 16-05-2024

Abstract: The rapid global spread of COVID-19 and RT-PCR tests are insensitive in early infection phases, according to hospitals. To find Covid-19, a fast, accurate test is needed. CT scans have shown diagnostic accuracy. CT scan processing using a deep learning architecture may improve illness diagnosis and treatment. A deep learning system for COVID-19 detection was derived using CT scan features. Using and comparing numerous transfer-learning models, fine-tuning, and the embedding process yielded the best infection diagnostic results. All models' diagnostic effectiveness was assessed using 2482 CT scan images. The optimized model demonstrated encouraging outcomes by significantly enhancing the sensitivity metric (86.26±1.72), a critical factor in accurately detecting COVID-19 infection. Additionally, the resulting model demonstrated elevated values for accuracy (81.15±0.17), specificity (77.90±1.33), precision (76.79±0.80), F1_score (81.24±0.37), and AUC (81.88±0.2). Deep learning methodologies have been effectively employed to detect COVID-19 in chest CT scan images. In the future, the suggested approach may be employed by clinical practitioners to study, identify, and effectively mitigate a greater number of pandemics.

Keywords: Deep learning, CT, Transfer learning, Lung, Classification, Diagnosis

1. Introduction

The World Health Organization (WHO) has classified the epidemic as a public health emergency of international concern [1]. There have been about 2.5 million confirmed coronavirus cases in Iraq until October 2023, with more than 25 thousand deaths, according to reports to the WHO. As of January 2020, Covid-19 has already spread to every corner of the globe. It is a leading cause of pneumonia and is easily spread from person to person [2]. According to data compiled by the WHO, the virus is responsible for a 2-3% fatality rate. To quickly identify and isolate infected individuals, it is crucial to do diagnostic tests using clinical symptoms and reverse-transcription polymerase chain reaction (RT-PCR). The sensitivity of the RT-PCR test may not be high enough to use it for early detection, however, as has been reported [3]. Computed tomography (CT) emerged as a noninvasive imaging method capable of identifying lung lesions linked to COVID-19 illness. Despite a positive finding on a chest CT scan, some patients' RT-PCR results came out negative. Inflammation and pneumonia in the lungs are often diagnosed through CT scans [4, 5]. Due to its superior categorization and feature extraction abilities, artificial intelligence (AI) based on machine learning (ML) and deep learning (DL) has achieved great success in the field of medical image interpretation [6]. The use of convolutional neural network (CNN) has increased in popularity for diagnosing pneumonia caused by viruses and distinguishing it from bacterial pneumonia in CT [7]. CNN is very effective in feature extraction, and it uses spatial filters to gather structural data.

M. Rahimzadeh *et al*. (2021) [8] suggested an accurate and rapid automatic approach for identifying COVID-19 via the images of chest CT scans of a patient. They provided a special dataset of 48,260 CT scan images from 282 healthy individuals and 15,589 CT scan images from 95 patients with COVID-19 infections. They came up with a new design to boost the performance of CNN in classification tasks. when applied to images that included minute items of significance. The architecture combined the Xception and ResNet50V2 models with a new feature pyramid network tailored for classification on over 7996 test images, the model obtained 98.49% accuracy. G. Zazzaro *et al.* (2021) [9] presented an assessment of the effectiveness of an automated COVID-19 detection system using CT scans of the chest as input to a transfer learning algorithm. They used a freely accessible multiclass CT scan dataset of 4171 CT images from 210 distinct patients. Features were extracted using CNNs that had been pre-trained on the ImageNet dataset. The retrieved features from the CT images and the collection of characteristics were selected using the information Gain filter. The resultant feature vectors were then used to train a set of k nearest neighbor (KNN) classifiers using 10-fold cross-validation to see how well each CNN classifies its obtained features. Overall accuracy in classifying was 99.04%.

using the test set's 414 images, which made up 10% of the whole dataset. Just 4 images from the test set were incorrectly categorized. S. Gupt *et al*. (2021) [10] used the SARS-COV2 dataset to identify normal images in addition to COVID-19 images. CT scans were used to detect whether or not a patient had a positive result for the COVID-19 viral imaging patterns. After having their characteristics extracted by several DL models, these images from the dataset were then passed to a variety of ML classifiers so that they could be classified as either COVID-19 images or normal images. According to the data, the combination combined with the logistic regression classifier in the VGG19 model yields not only the greatest possible area under the curve (AUC) but also the highest possible accuracy of 94.5%. A. Ardakani *et al.* (2020) [11] offered a quick and reliable approach for diagnosing COVID-19 based on AI hundred and twenty (CT) slices from a total of 108 patients with laboratory-confirmed COVID-19 and 86 patients with other atypical and viral pneumonia diseases were included in the COVID19 group. Ten popular CNNs (VGG-19, AlexNet, VGG-16, SqueezeNet, GoogleNet, MobileNet-V2, ResNet-50, ResNet-18, ResNet-101, and Xception) were used to classify individuals as infected with COVID-19 or not. For overall performance, the best networks were Xception and ResNet-101. ResNet-101 distinguished COVID-19 patients from non-COVID-19 cases with an AUC of 0.994, a sensitivity of 100%, a specificity of 99.02%, and an accuracy of 99.51%. 100% sensitivity, 100% specificity, and 99.02% accuracy were achieved using Xception, yielding an AUC of 0.994. The radiologist achieved an AUC of 0.873, 89.21% sensitivity, 83.33% specificity, and 86.27% accuracy. S. Srete *et al.* (2021) [12] offered a technique for categorizing COVID-19 and typical CT volumes that makes use of AI. Using a DL model known as ResNet-50, The proposed AI system makes COVID-19 predictions on all CT images that make up a 3D CT scan. Finally, the AI technique utilizes imaging-level predictions to make a COVID-19 diagnosis in a 3D CT volume. Demonstrate that the suggested DL model achieves an AUC value of 96% when applied to the problem of detecting COVID-19 from CT images. S. Biswas *et al.* (2021) [13] developed a transfer learning and chest CT scan, and a prediction model for COVID-19. Initially, COVID-19 was predicted by using three distinct DL models, namely VGG-16, ResNet50, and Xception. Every one of these variations is regarded as a regular option. After that, a strategy for integrating the pre-trained models that were described before was proposed to enhance the capability of the system as a whole to generate correct predictions. This was done to enhance the system, an alternative model is suggested to obtain an accuracy of classification of 98.79% when using the dataset of SARS-CoV-2 CT that is available to the general public. Moreover, the model has a high F1_score of 0.99%. The objective of this work is to develop and implement a reliable system for the detection and classification of COVID-19 using image processing and DL methods to achieve a high level of classification accuracy. The remainder of this research is broken down as follows: Section 2 details the methodology behind the DL framework. Section 3 presents the dataset, including information and performance assessment indicators, and describes the conversations that ensued. Section 4 shows the results and discussion, while the conclusions are presented in Section 5.

2. Materials and Methods

2.1 VGG16

The visual geometry group (VGG) of the university of Oxford's department of engineering science developed a DL model called VGG 16 for image classification. It contains over 144 million parameters and 16 layers (13 convolutional and 3 fully connected), and Figure. 1 shows the VGG16 model architecture. This increases the model's ability to capture localized characteristics that are unique to a certain class. Using tiny kernel sizes in the VGG architecture does not come without its downsides.

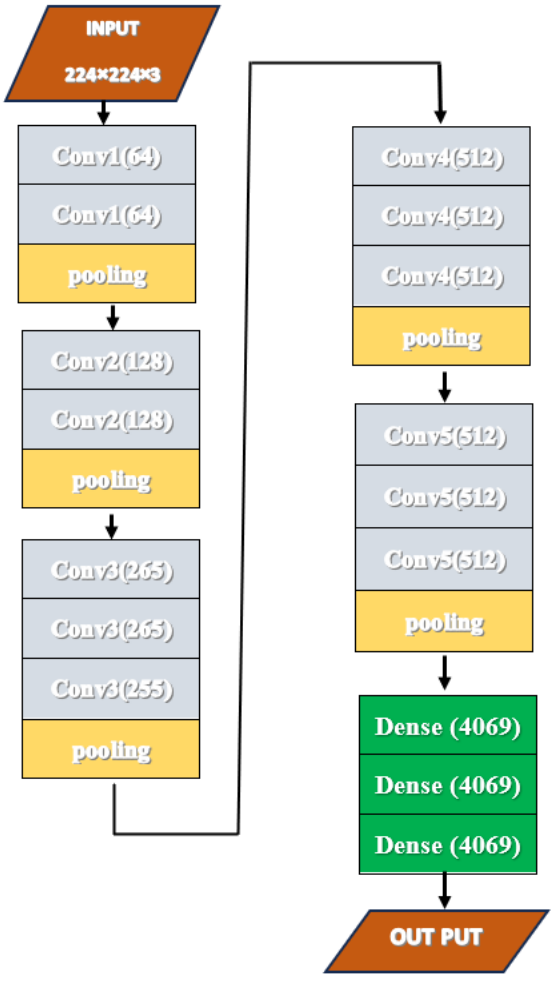

Figure1. VGG16 model architecture

The number of trainable parameters in the VGG model rises due to the tiny size of the convolutions used therein. Additionally, it makes use of pooling layers in strategic locations to filter out superfluous characteristics and simplify the model [14].

2.2 Transfer Learning, Fine-Tuning, and Embedding

Training and testing phases may leverage various domains, tasks, and/or data distributions via the use of ML techniques known as transfer learning (TL), inductive transfer, knowledge transfer, or learning to learn [15]. The goal of TL is to use the insights gained by analyzing one issue to the resolution of another, comparable but unique problem [16]. Since the size of most new datasets is not large enough to train an appropriate model from the start, this transferred information may be used in the new dataset. Different variables between the source and the target domains and tasks have led to the definition of three primary TL sub-areas [17]. The last step in a CNN's training process is to retrain the network's "brain" to detect new classes of objects for which it was not originally designed. A multi-stage procedure including Fine-tuning in Keras was employed in this study. Backpropagation's reverse pass is prevented from reaching the network's head by, first, freezing all layer's underneath it. Second, the network's terminal nodes are disconnected and replaced with fresh, initialized nodes. After all layer heads are linked, training may begin. The main advantage of the embedding approach is that it can construct complex patterns that are very robust to changes in distortion, occlusion, and lighting [18]. Furthermore, for limited datasets, this approach reduces training time and result variability Using embedding vectors to represent input CT images is another way to use the pre-trained CNN architectures. Conventional ML models are trained with the data after the feature vectors are created using techniques like random forest and support vector machine. This is accomplished by CNN by summing all attribute values in the final layer. Training times are shortened and outcomes are more consistent, even with modest data sets, thanks to this method [19].

2.3 Hyper-Parameter Tuning

The performance of CNN is influenced by crucial characteristics known as hyper-parameters. These hyper-parameters include many elements such as the number of layers, learning rate, optimization approach, and activation functions. The purpose of this adjustment is to optimize the hyper-parameters of the model to get improved discriminatory abilities. In the present study, we conducted training The hyper-parameter tuning process for the five DL models resulted in the identification of the ideal configuration [20]. All individuals undergo a comprehensive training program to enhance their skills and abilities. On many occasions, the hyper-parameter values were altered to observe their impact. Initially, the models were updated by including a variety of trainable layers. Training a neural network requires fine-tuning a wide variety of parameters and hyperparameters. Examples include the learning rate, batch size, batch normalization, image resolution, data augmentation techniques, and so on. Tuning parameters is an iterative process that requires several trials to get a good outcome. The process of identifying optimal parameters for a given problem is itself an optimization problem. Therefore, several iterations and trials are performed during this process to find hyperparameters that provide passable results [21]. The concept of batch size pertains to the practice of partitioning data into batches prior to its transmission to the network. An alternative perspective is considering the quantity of training samples processed during a single forward/backward pass. An increase in batch size necessitates a corresponding increase in memory space. In the proposed system, the batch size is determined to be 32. This choice is motivated by the observation that lower batch sizes tend to expedite the training process of the network and need a lesser amount of memory resources. Moreover, if all samples are used simultaneously during propagation, the network parameters will undergo a single update. Various additional factors may be considered, depending on the context, such as the number of layers, the size of the lines that make up those layers, the layer capacity, the number of nodes (neurons), and so on. Incorrectly describing these parameters may lead to an overfitting or underfitting model, making the definition of the Hyperparameter one of the most critical issues confronting any researcher working in the area of neural network design. Overfitting or underfitting might occur if these settings are specified incorrectly. the behavior of the CNN model parameters is provided in the following sections [22]. The hyperparameter used in this work was as follows: The loss function is the cross-entropy of categories. With an initial learning rate of 0.001, with Adam serving as an optimizer, Dataset divided by 80% training and 20% testing, 100 epochs are the maximum allowed. The training data was divided into 32 batches.

3. Dataset and Work Environment

The Python programming language was used for this study. The Python library uses Keras, which is a no-cost, open-source Python library for DL that is compatible with TensorFlow. It also works with the Python scientific and numerical libraries NumPy and SciPy. We have implemented this by using Colab notebooks from Google via computer specifications: Processor: Intel(R) Core (TM) i5-8265U CPU @ 1.60 GHz, RAM: 800 GB, 64-bit operating system. x64-based processor. Once a dataset has been collected, it must undergo pre-processing to conform to the requirements of the proposed model. The initial step in using images is the pre-processing stage when key image

characteristics are shown. Here, we discuss ways in which the initial CT datasets have been enhanced. These improvements may be used for a wide range of problems, such as expanding the dataset and addressing the problem of insufficient training data in COVID-19 images, decreasing noise, and assessing its impact on training deep CNN models [23]. In the last step of preprocessing, the raw dataset is subdivided into a smaller subset that will be used to train and test the proposed system [24]. In this work, the preprocessing used data augmentation, image normalization, and image resizing. The use of deep convolutional models in our work necessitates a substantial quantity of images for training to enhance performance while mitigating the risk of overfitting. However, the quantity of images inside our collection is inadequate. The system's robustness will increase in proportion to the diversity of the training data. Data augmentation was used to enlarge the quantity of training images as well as enhance the diversity among these images. Additionally, this aids in improving the accuracy of predictions and mitigating the issue of overfitting. To enhance the dataset, we used several transformation techniques, including rotation, flipping, shearing, and zooming. The rotation angle was randomly selected from a range of 0 to 30 degrees. The range of random zooming was between 90% and 110%.

This present work introduces publicly available image datasets that contain CT images [25]. All of the data used in this article were taken directly from Kaggle's open data repository. They collected 2482 images of the first data set has a descriptive name: SARS-COV-2. All of the images are JPGs, with the largest being 534 x 341 pixels and the smallest measuring 244 x 145 pixels. two evaluate DL representations on two sets to learn about the classification's generalizability and its efficacy in retrospective investigations using patient demographic data. Only axial CT volumes were taken into account for both patients. Here is a rundown of the data sets: SARS-CoV-2 CT scan data set [26]. Over 4,173 thoracic CT slices, 210 patients are depicted. Eighty individuals were found to have SARS-CoV-2 infection (2,168 CT slices) and fifty were found to be virus-free (757 CT slices). Patients with various lung disorders were excluded from the study, making up the remaining 80 cases. The radiological findings were utilized to manually choose the most relevant CT slice for each CT volume to be used as input for DL. Patients' SARS-CoV-2 status was validated by RT-PCR testing, and the dataset was compiled from hospitals in Sao Paulo, Brazil. As a result, the automated patient categorization provided by DL models is probably skewed toward spotting cases that are also detected by the RT-PCR test. Since all of the radiological abnormalities found by the experts were on the most diagnostically relevant CT slice, we were able to eliminate this bias in our study.

4. Architecture of Model and Evaluation Parameters

The purpose of this research is to develop an automated system that makes use of a hybrid technique that combines DL, in the form of a CNN, and a ML algorithm, such as a support vector machine (SVM) and XGBoost. The chest CT scans of COVID-19 patients are going to be analyzed with the hope of precisely identifying people with the disease. To derive DL characteristics, the approach under consideration makes use of a CNN architecture. To be more specific, the CNN layers—not the fully linked layers—are the ones that are employed for feature extraction. After that, classification is carried out with the use of both ML classifiers and DL classifiers. The model's foundational layers are constructed at this step. The number of initial convolution layers is a key component of the design process. To extract the feature map and choose the best feature based on the pooling layer, numerous convolution and pooling layers would need to be applied to the (i, j) 300x300 input images.

As a first step, we developed the recommended model. To find the best features to extract from the feature maps that emerged from the convolution layer, 13 layers were used, including 6 convolutional layers, 6 batch regularization layers, 6 activation function (ReLU) levels, and 5 max pooling layers. After passing through a series of layers such as convolution, batch normalization, nonlinear, and pooling, the data enters the FC stage, also known as the classification stage, when it is reduced to a single feature vector in one dimension (1D). the process of feature extraction will be conducted by DL techniques. Subsequently, for the classification task, the fully connected layers will be substituted with ML methods used in this research, namely SVM and XGBoost. and DL method Figure. 2 provides an elucidation of the functioning of the hybrid model.

AUC, accuracy, precision, sensitivity, and F1_score were used to compare the performance of several classifiers used in the SARS-COV-2 dataset's image classification. The percentage of successfully classified images as COVID-19 might be used as an indicator of how accurate the system is. Precision, in a similar vein, might be thought of as making correct forecasts about the whole [27]. The equations allow for the determination of these parameters.

$$\text{Accuracy} = \frac{\text{TP+TN}}{\text{TP+TN+FP+FN}} \quad (1)$$

$$\text{sensitivity} = \frac{\text{TP}}{\text{TP+FN}} \quad (2)$$

$$\text{Precision} = \frac{\text{TP}}{\text{TP+FP}} \quad (3)$$

$$\text{F1\_score} = 2 \times \frac{\text{Precision} \times \text{Recall}}{\text{Precision+Recall}} \quad (4)$$

$$\text{Specificity} = \frac{TN}{TN+FP} \quad (5)$$

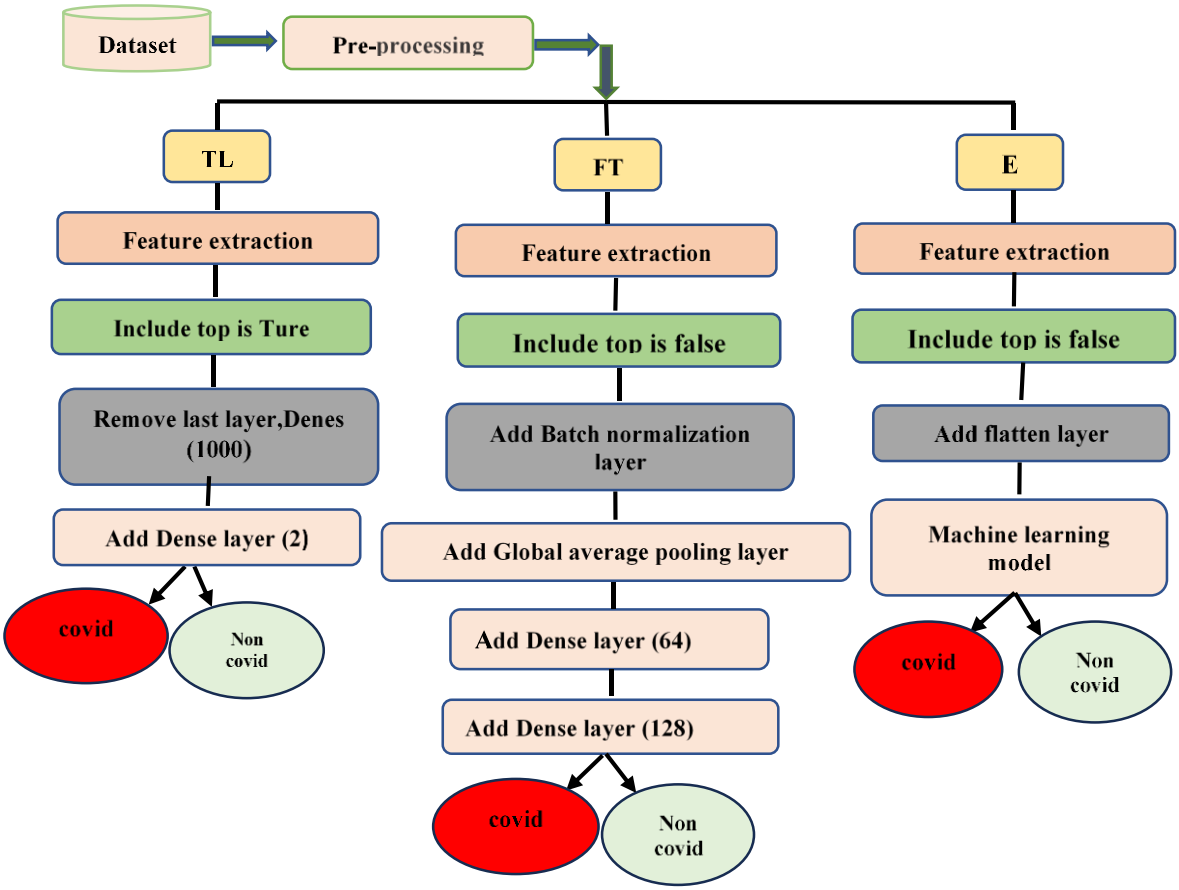

Figure 2. The Architecture of the Training Model

where, the abbreviations for True Positive, True Negative, False Positive, and False Negative are (TP), (TN), (FP), and (FN) respectively.

5. Results and Discussion

Here, we provide the findings from our effort to categorize lung types, as well as comparisons to previous studies in the field. The first model, the TL proposed model takes a CT scan image with dimensions of 224×224×3 as input to the output of the probabilistic results from the last layer of the network. The CNN performance is determined by the following performance metrics: accuracy, sensitivity, specificity, precision, F1_score, and AUC, as shown in Figure. 3. Then, the TL model achieved after calculating the confusion matrix on the testing set the results were respectively as follows: 73.52±6.69, 58.58±2.75, 86.44±8.45, 80.25±4.24, 64.86±1.52 and 72.5±7.87. The variations in the training loss function show the Adam algorithm's normal behavior. The VGG16 model was used by adding feature extraction Then making trainable layers false and including the top true after that removing the last layer Denes (1000) without a fully connected classifier / layers, and adding classifier Denes (2) to it by COVID and non-COVID as shown in Figure. 2.

The second model (FT model) has modified the TL model, but after removing all classifier layers (including top is false). Then, we added a batch normalization layer, a Global average pooling layer, and three blocks: Dense layer (64), Dense Layer (128), and Dense (2), as shown in Figure. 2. Figure. 4 shows the training accuracy, validation accuracy, and loss retractions and ROC of the proposed CNN model trained on the CT scan dataset by using FT. The parameters were modified and a model was produced that gave a higher accuracy than the one implemented in TL; it was 81.15±0. 17, and sensitivity, specificity, precision, F1_score, and AUC as: 86.26±1.72, 77.90±1.33, 76.79±0.80, 81.24±0.37, 81.88±0.2, respectively. It indicates that the development that is made to the model gives good results.

In the third model (embedding), the VGG16 model was used as a feature extractor, as shown in Figure. 2. The model was built according to this method, making the trainable layer false, including tope false, adding a flattening layer, and sequentially adding the ML model. The ML model was implemented using two distinct algorithms. The first model used was XGbost, followed by the subsequent utilization of SVM. In both instances, the outcomes exhibited limited strength as compared to the use of prior methodologies, as shown in Figure. 5. The results show for the E_XGbost classifier that accuracy, sensitivity, specificity, precision, F1_score, and AUC were: 49.05±3.14, 49.04±6.37, 49.06±1.47, 45.19±3.33, 47.00±4.69, and 50.32±5.29, respectively.

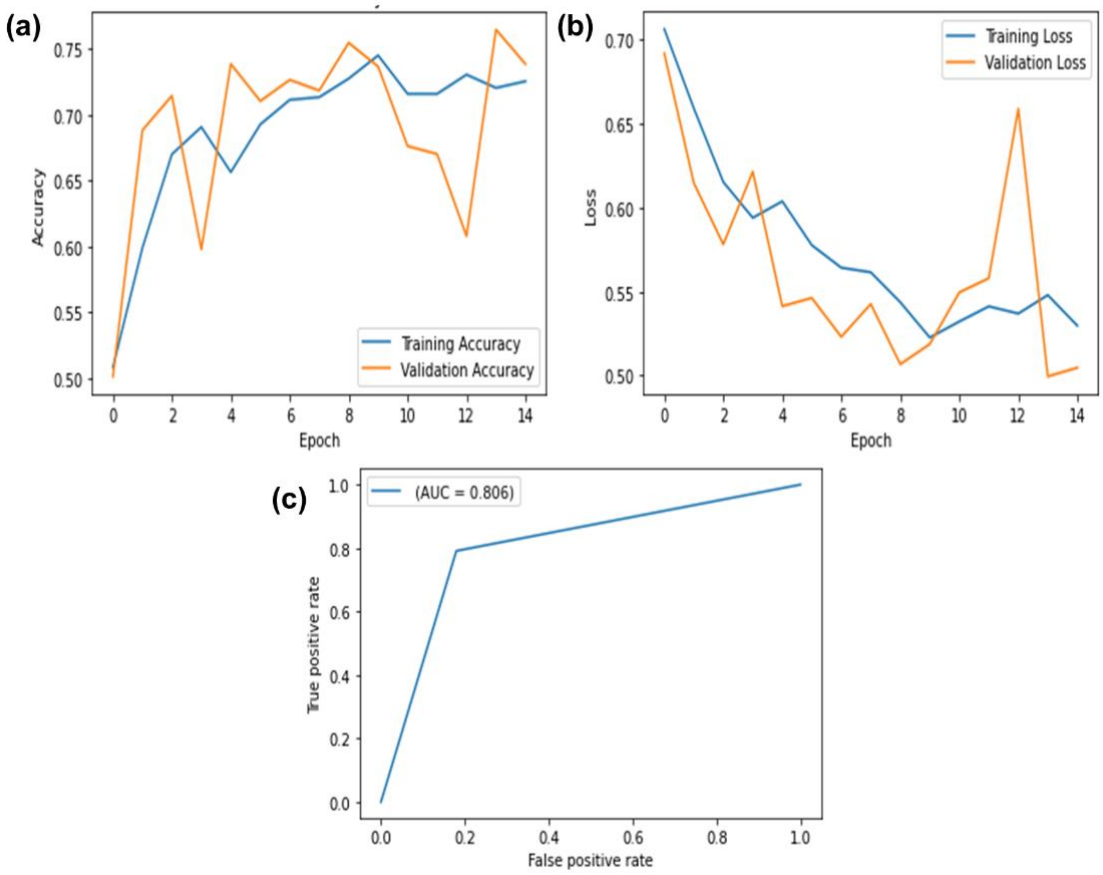

Figure 3. TL model results using SARS-CoV-2: (a), accuracy (b) loss, and (c) ROC curve

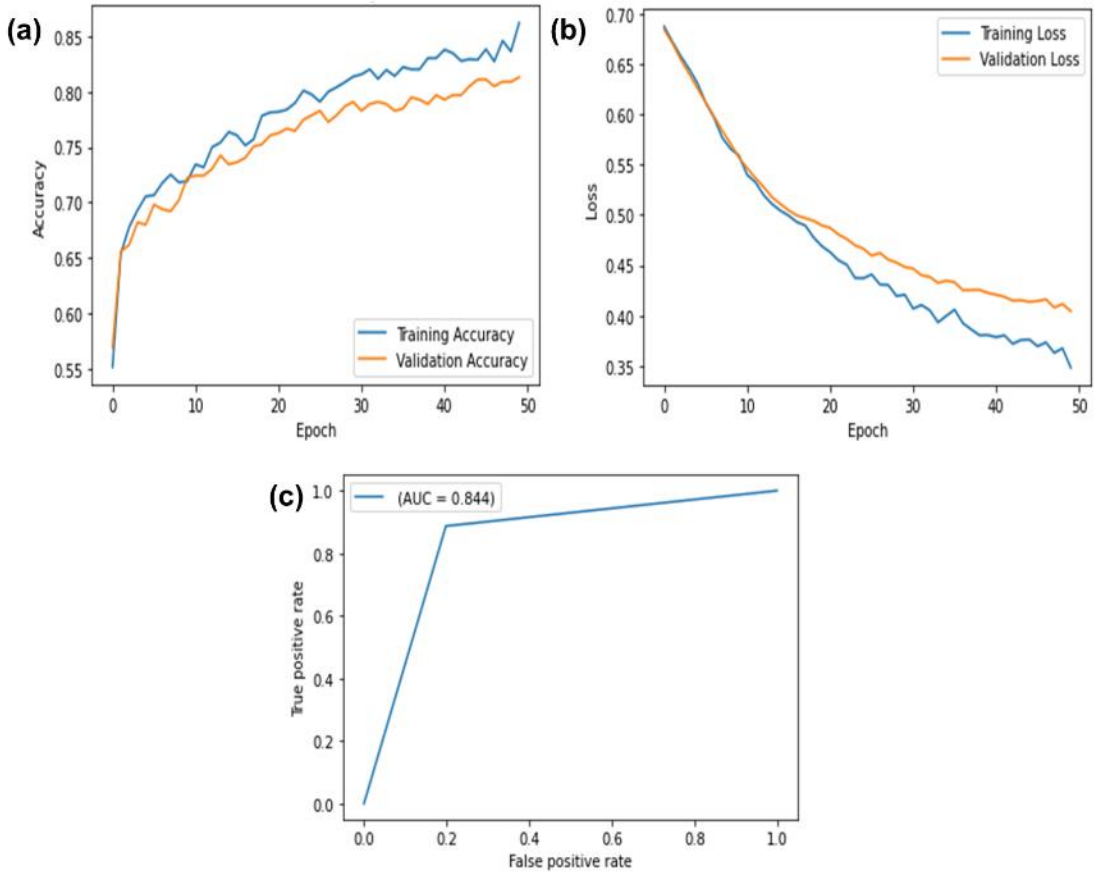

Figure 4. FT model results using SARS-CoV-2: (a), accuracy (b) loss, and (c) ROC curve

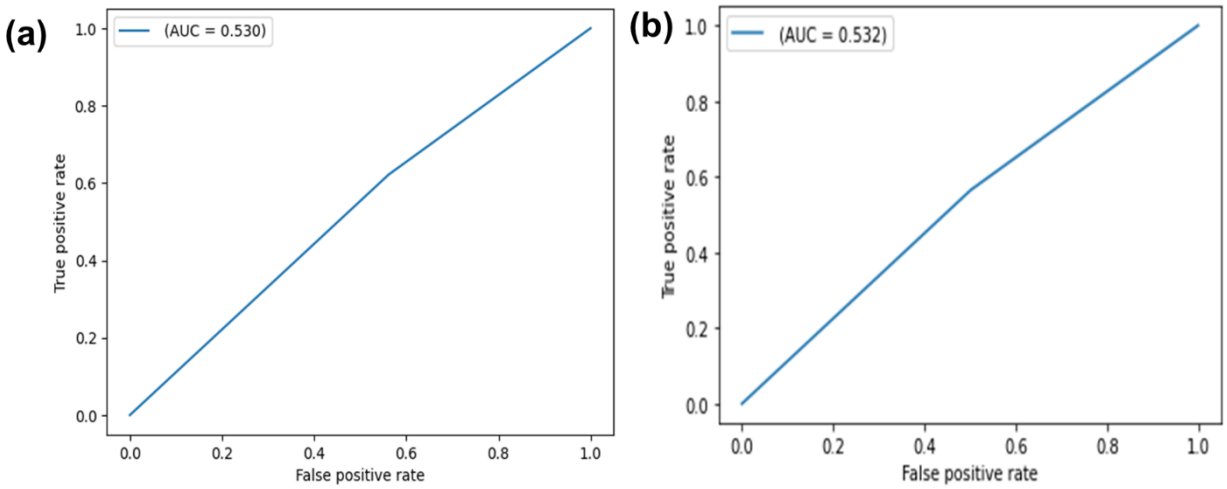

Figure 5. Embedding model ROC curve using SARS-CoV-2: (a) XGbost (b) SVM

Table 1. Results for all methods

method	accuracy	sensitivity	specificity	precision	F1_score	AUC
TL	73.52±6.69	58.58±2.5	86.44±8.45	80.25±4.24	64.86±1.52	72.5±7.87
FT	81.15±0.17	86.26±1.72	77.90±1.33	76.79±0.80	81.24±0.37	81.88±0.2
E_XGbost	49.05±3.14	49.04±6.37	49.06±1.47	49.06±1.47	47.00±4.69	50.32±5.29
E_SVM	50.30±1.88	57.82±4.75	43.82±4.54	46.99±1.69	51.79±2.53	50.82±1.88

Table 2. Comparison with other studies

Ref.	Method	accuracy	sensitivity	specificity	precision	F1_score	AUC
Rahimzadeh *et al*. [8]	Xception	98.49	94.96				
	ResNet50V2	96.55	98.02				
Gupt *et al*. [10]	VGG19	93.90	93.90		93.90	94.00	0.981
	VGG16	94.20	94.20		94.20	94.20	0.982
Ardakani *et al*. [11]	VGG-19	85.29	92.16	87.43			0.943
	AlexNet,	79.92	89.21	68.63			0.890
	VGG-16 SqueezeNet	83.33	80.39	86.27			0.926
	GoogleNet,	82.84	87.43	87.25			0.899
	MobileNetV2 ResNet-50, ResNet-18, ResNet-101, Xception	85.29	81.37	90.20			0.927
		92.16	97.06	87.25			0.982
		94.12	90.20	100			0.990
		91.91	95.87	88.23			0.975
		99.51	100	99.02			0.994
		99.02	98.04	100			0.994
Biswas *et al*. [13]	VGG-16, ResNet50 Xception	98.79	98.39		98.39	98.39	0.983
		95.17	95.17		95.17	95.17	0.951
		94.57	94.57		94.57	94.57	0.945
Our model	TL	73.52±6.69	58.58±2.50	86.44±8.45	80.25±4.24	64.86±1.52	72.50±7.87
	FT	81.15±0.17	86.26±1.72	77.90±1.33	76.79±0.80	81.24±0.37	81.88±0.2
	E_XGbost	49.05±3.14	49.04±6.37	49.06±1.47	49.06±1.47	47.00±4.69	50.32±5.29
	E_svm	50.30±1.88	57.82±4.75	43.82±4.54	46.99±1.69	51.79±2.53	50.82±1.88

while the E_SVM classifiers were: 50.30±1.88, 57.82±4.75, 43.82±4.54, 46.99±1.69, 51.79±2.53, and 50.82±1.88, respectively. It is noticed from the embedding method that when DL and ML are combined, the execution speed of the model is higher, but the accuracy is lower compared to the TL and FT models.

Table 1 shows the results for all of the metrics that were computed, including accuracy, sensitivity, specificity, F1-score, precision, and AUC. The findings demonstrated that the second approach (FT) obtained better results in comparison to those obtained using

other methods. while the third approach is regarded as having the lowest performance of the methods.

In the last section, Table 2 presents a comprehensive summary of the results from several experiments done on the diagnostic system for COVID-19. The assessment was based on the correctness of the comparison. It is important to emphasize that direct comparisons are unfeasible owing to the discrepancies between the data sets, such as variations in the number of images and different methodologies used. However, when compared to earlier works, our study achieved superior results, reliability, and resilience for the present model.

6. Conclusions

In this work, a VGG16 model as DL has been developed for the diagnosis of COVID-19 from chest CT scan images. The modified model has been compared with other existing models. The tuned model showed promising results by increasing the sensitivity value (86.26±1.72), which is crucial and important in diagnosing COVID-19 infection. Also, the model obtained high values for accuracy (81.15±0.17), specificity (77.90±1.33), precision (76.79±0.80), F1_score (81.24±0.37), and AUC (81.88±0.2). DL approaches have been implemented successfully to detect COVID-19 in chest CT scan images. DL in the area of radiology has achieved superior achievement. In the future, clinical doctors can use the proposed method to analyze, identify, and prevent pandemics, subsequently managing pandemics more effectively.

References

[1] Y. Karadayi, M.N. Aydin, A.S. Oğrencí, Unsupervised Anomaly Detection in Multivariate Spatio-Temporal Data Using Deep Learning: Early Detection of COVID-19 Outbreak in Italy. IEEE Access, 8, (2020) 164155-164177. https://doi.org/10.1109/ACCESS.2020.3022366

[2] R.G. Babukarthik, V.A.K. Adiga, G. Sambasivam, D. Chandramohan, J. Amudhavel, Prediction of COVID-19 Using Genetic Deep Learning Convolutional Neural Network (GDCNN). IEEE Access, 8, (2020) 177647-177666. https://doi.org/10.1109/ACCESS.2020.3025164

[3] P. Bhowal, S. Sen, J.H. Yoon, Z.W. Geem, R. Sarkar, Choquet Integral and Coalition Game-Based Ensemble of Deep Learning Models for COVID-19 Screening from Chest X-Ray Images. IEEE Journal of Biomedical and Health Informatics, 25(12), (2021) 4328-4339. https://doi.org/10.1109/JBHI.2021.3111415

[4] E. Acar, E. Şahin, İ. Yılmaz, improving effectiveness of different deep learning-based models for detecting COVID-19 from computed tomography (CT) images. Neural Computing and Applications, 33(24), (2021) 17589-17609. https://doi.org/10.1007/s00521-021-06344-5

[5] M.Y. Kamil, (2016) Morphological gradient in brain magnetic resonance imaging based on intuitionistic fuzzy approach. in Al-Sadiq International Conference on Multidisciplinary in IT and Communication Techniques Science and Applications, AIC-MITCSA, IEEE, Iraq. https://doi.org/10.1109/AIC-MITCSA.2016.7759924

[6] J.C. Clement, V. Ponnusamy, K.C. Sriharipriya, R. Nandakumar, A Survey on Mathematical, Machine Learning and Deep Learning Models for COVID-19 Transmission and Diagnosis. IEEE Reviews in Biomedical Engineering, 15, (2022) 325-340. https://doi.org/10.1109/RBME.2021.3069213

[7] Y. Oh, S. Park, J.C. Ye, Deep Learning COVID-19 Features on CXR Using Limited Training Data Sets. IEEE Transactions on Medical Imaging, 39(8), (2020) 2688-2700. https://doi.org/10.1109/TMI.2020.2993291

[8] M. Rahimzadeh, A. Attar, S.M. Sakhaei, A fully automated deep learning-based network for detecting COVID-19 from a new and large lung CT scan dataset. Biomedical Signal Processing and Control, 68, (2021) 102588. https://doi.org/10.1016/j.bspc.2021.102588

[9] G. Zazzaro, F. Martone, G. Romano, L. Pavone, A Deep Learning Ensemble Approach for Automated COVID-19 Detection from Chest CT Images. Journal of Clinical Medicine, 10(24), (2021) 5982. https://doi.org/10.3390/jcm10245982

[10] S. Gupta, P. Aggarwal, N. Chaubey, A. Panwar, Accurate Prognosis of Covid-19 Using Ct Scan Images with Deep Learning Model and Machine Learning Classifiers. NIScPR-CSIR, 50(1), (2021) 19-24.

[11] A.A. Ardakani, A.R. Kanafi, U.R. Acharya, N. Khadem, A. Mohammadi, Application of deep learning technique to manage COVID-19 in routine clinical practice using CT images: Results of 10 convolutional neural networks. Computers in Biology and Medicine, 121, (2020) 103795, 2020. https://doi.org/10.1016/j.compbiomed.2020.103795

[12] S. Serte, H. Demirel, Deep learning for diagnosis of COVID-19 using 3D CT scans. Computers in Biology and Medicine, 132, (2021) 104306. https://doi.org/10.1016/j.compbiomed.2021.104306

[13] S. Biswas, S. Chatterjee, A. Majee, S. Sen, F. Schwenker, R. Sarkar, Prediction of COVID-19 from Chest CT Images Using an Ensemble of

Deep Learning Models. Applied Sciences, 11(15), (2021) 7004. https://doi.org/10.3390/app11157004

[14] E. Jangam, A.A.D. Barreto, C.S.R. Annavarapu, Automatic detection of COVID-19 from chest CT scan and chest X-Rays images using deep learning, transfer learning and stacking. Applied Intelligence, 52, (2022) 2243–2259. https://doi.org/10.3390/app11157004

[15] M.Y. Kamil, A.L.A. Jassam, Analysis of Tissue Abnormality in Mammography Images Using Gray Level Co-occurrence Matrix Method. Journal of Physics: Conference Series, 1530, (2020). https://doi.org/10.1088/1742-6596/1530/1/012101

[16] N.N. Das, N. Kumar, M. Kaur, V. Kumar, D. Singh, Automated deep transfer learning-based approach for detection of COVID-19 infection in chest X-rays. Irbm, 43(2), (2022) 114-119. https://doi.org/10.1016/j.irbm.2020.07.001

[17] J. Mantas, setting up an easy-to-use machine learning pipeline for medical decision support: a case study for COVID-19 diagnosis based on deep learning with CT scans. Public Health Dur. Pandemic, 272, (2020) 13.

[18] R.R. Kadhim, M.Y. Kamil, Comparison of machine learning models for breast cancer diagnosis. IAES International Journal of Artificial Intelligence, 12(1), (2023) 415-421. http://doi.org/10.11591/ijai.v12.i1.pp415-421

[19] A.F. Mahmood, S.W. Mahmood, Auto informing COVID-19 detection result from x-ray/CT images based on deep learning. Review of Scientific Instruments, 92(8), (2021). https://doi.org/10.1063/5.0059829

[20] A.S. Obaid, M.Y. Kamil, B.H. Hamza, People identification via tongue print using fine-tuning deep learning. International Journal of Reconfigurable and Embedded Systems, 12(3), (2023) 433-441. http://doi.org/10.11591/ijres.v12.i3.pp433-441

[21] M. Abdel-Basset, H. Hawash, N. Moustafa, O.M. Elkomy, Two-stage deep learning framework for discrimination between COVID-19 and community-acquired pneumonia from chest CT scans. Pattern recognition letters, 152, (2021) 311-319. https://doi.org/10.1016/j.patrec.2021.10.027

[22] A.K. Reyes, J.C. Caicedo, J.E. Camargo, Fine-tuning Deep Convolutional Networks for Plant Recognition. CLEF (Working Notes), 1391, (2015) 467-475.

[23] I. Ahmed, A. Ahmad, G. Jeon, An IoT-Based Deep Learning Framework for Early Assessment of Covid-19. IEEE Internet of Things Journal, 8(21), (2021) 15855-15862. https://doi.org/10.1109/JIOT.2020.3034074

[24] K. Misztal, A. Pocha, M. Durak-Kozica, M. Wątor, A. Kubica-Misztal, M. Hartel, The importance of standardisation–COVID-19 CT & Radiograph Image Data Stock for deep learning purpose. Computers in Biology and Medicine, 127, (2020) 104092. https://doi.org/10.1016/j.compbiomed.2020.104092

[25] H.S. Alghamdi, G. Amoudi, S. Elhag, K. Saeedi, J. Nasser, Deep Learning Approaches for Detecting COVID-19 From Chest X-Ray Images: A Survey. IEEE Access, 9, (2021) 20235-20254. https://doi.org/10.1109/ACCESS.2021.3054484

[26] J. Ruano, J. Arcila, D. Romo-Bucheli, C. Vargas, J. Rodríguez, O. Mendoza, M. Plazas, L. Bautista, J. Villamizar, G. Pedraza, A. Moreno, D. Valenzuela, L. Vázquez, C. Valenzuela-Santos, P. Camacho, D. Mantilla, F. Martínez Carrillo, Deep learning representations to support COVID-19 diagnosis on CT slices. Biomedica, 42(1), (2022) 170-183. https://doi.org/10.7705/biomedica.5927

[27] E.A. Radhi, M.Y. Kamil, Breast Tumor Detection Via Active Contour Technique, International Journal of Intelligent Engineering and Systems, 14(4), (2021) 561-570. https://doi.org/10.22266/ijies2021.0831.49

Acknowledgments
The authors would like to thank Mustansiriyah University for their valuable support and for providing essential facilities for this research.

Authors Contribution Statement
Marwa A. Shames- Investigation, Formal analysis, Writing—original draft and Writing-review, editing. Mohammed Y. Kamil - Conceptualization, Methodology, Software, Validation and Writing-review, editing. Both the authors read and approved the final version of the manuscript.

Funding
No funding was received for this research work.

Conflicts of Interest
The authors declare no conflict of interest.

Data Availability
Data is public on the Kaggle website, https://forms.gle/zNF3zVWu2k6ztELP8

Has this article screened for similarity?
Yes